Journal of Magnetism and Magnetic Materials 385 (2015) 428–432

Contents lists available at ScienceDirect

Journal of Magnetism and Magnetic Materials

journal homepage: www.elsevier.com/locate/jmmm

Pressure–temperature phase diagram of CeAg

Hiroyuki Hidaka*, Shinya Otani, Hiraku Saito, Kaori Tatsumi, Tatsuya Yanagisawa, Hiroshi Amitsuka

Department of Physics, Hokkaido University, Sapporo 060-0810, Japan

ARTICLE INFO

Article history:
Received 2 February 2015
Received in revised form
12 March 2015
Accepted 14 March 2015
Available online 17 March 2015

Keywords:
CeAg
Pressure–temperature phase diagram
Ferromagnetic order
Structural phase transition
Kondo effect

ABSTRACT

We have performed electrical-resistivity measurements under hydrostatic pressures ranging up to 4.47 GPa on the cubic compound CeAg. A pressure–temperature phase diagram has been revised in a high-pressure range above ~2.1 GPa, where the system is known to enter into an unidentified phase through a first-order phase transition. We have found that the electrical resistivity shows a clear kink anomaly below ~ 4 K in this unknown phase. The anomaly shifts to lower temperature with increasing pressure, and shows a tendency to reach absolute zero at ~6 GPa, suggesting the presence of a pressure-induced quantum critical point around this pressure. We have also observed that a first-order phase boundary line, which separates the phase diagram into two regions of a tetragonal phase and the unidentified phase, seems to terminate in a critical end point located at (P_{CEP}, T_{CEP}) ~(3.2 GPa, 200 K). This suggests that the crystal symmetry of the unidentified phase above ~2.1 GPa is also tetragonal.

1. Introduction

The CsCl-type cubic compound CeAg is known as an archetypal ferroquadrupole (FQ) ordering system. At ambient pressure, the 4*f* electrons of this system undergo the FQ order at $T_Q \sim 16$ K [1–4]. Applying hydrostatic pressure (P) interrupts the FQ order at a very weak pressure of 0.2 GPa, where a first-order phase transition takes place at $T_{s1} \sim 40$ K with a thermal hysteresis in electrical resistivity ρ [5–8]. T_{s1} increases linearly at a rate of ~160 K/GPa with increasing pressure [5–8]. This pressure-induced transition has been interpreted as a structural phase transition from cubic to tetragonal due to a band Jahn–Teller effect in a Ce 5d_{eg} band, by analogy with the behavior seen in $RAg_{1-x}In_x$ systems (R=La, Ce, and Pr) [6,7,9–18]. It is known that the electronic density of states (DOS) of the RAg systems has a sharp peak structure due to R-5*d* and Ag-4*p* orbits just above the Fermi level [19–24]. Both applying pressure and doping In ions raise the Fermi level to the peak position of the DOS, and may induce the cubic-to-tetragonal crystal deformation, so that the system gains the electronic energy by lifting the 5*d*-band degeneracy [9,7,25]. Interestingly, in the higher pressure range of $P > \sim 2$ GPa, CeAg exhibits another first-order phase transition with a large temperature hysteresis, whose transition temperature T_{s2} shows a similar pressure dependence to that of T_{s1} [5,7,8].These similarities suggest that this transition is also associated with a structural change [5,7,8]. At present, however, it is not clear what phase actually appears below T_{s2} and how the phase boundary line behaves at low temperatures.

In addition to these three phase transitions, CeAg undergoes a ferromagnetic (FM) ordering at $T_C = 5.5$ K below T_Q at ambient pressure [2,4]. The neutron diffraction experiments have revealed that the crystal structure at 1.8 K is tetragonal with the c/a ratio of 1.019 ±0.001 [26]. The magnetic easy axis is along the tetragonal [001] axis, and the ordered moment has been estimated to be ~0.8 μ_B/Ce [4,26]. It is known that as the pressure is applied in the pressure range below 2 GPa, T_C initially increases with a tiny step at around 0.2 GPa, where the T_{s1} transition takes place, and then decreases, showing a rounded maximum at ~0.7 GPa [5–8,27,28]. However, the pressure dependence of T_C above 2 GPa has long been controversial; the ρ measurements by Eiling and Schiling and the ac-susceptibility χ_{ac} measurements by Cornelius et al. have shown that T_C continues to decrease monotonously [5,27], while the ρ measurements by Kurisu have argued that T_C starts increasing above ~2 GPa [7].

The variety of low-temperature phases mentioned above implies that CeAg provides a unique example for studying the interplay between the structural change and the 4*f*-electronic states involving magnetic-dipole and electric-quadrupole correlations. However, it has not been clarified yet how the two first-order phase transitions influence the 4*f* states under pressure. It will also be of great interest that the system appears to be approaching the FM quantum critical region with applying pressure, promising the emergence of exotic states as found recently in various FM systems [29–32]. However, as described above, even a pressure-temperature (P-T) phase diagram of this compound has not been settled

* Corresponding author.
E-mail address: hidaka@phys.sci.hokudai.ac.jp (H. Hidaka).

http://dx.doi.org/10.1016/j.jmmm.2015.03.054
0304-8853/

yet, especially in the range above ~2 GPa. In the present study, we have performed the electrical-resistivity measurements on CeAg under high pressure up to 4.47 GPa in order to construct a reliable P–T phase diagram and investigate a possible FM quantum critical point for the 4f-electron systems.

2. Experimental procedure

A polycrystalline CeAg ingot was prepared by arc-melting the constituents, and annealed for 7 days at 500 °C. We have performed the $\rho(T)$ measurements on the annealed polycrystalline sample under high pressure ranging up to 4.47 GPa. Since the sample is oxidized rapidly in air, we kept it in Ar–gas atmosphere by using a glove bag during the sample installation in a pressure cell. $\rho(T)$ was measured by means of a conventional four prove method in the temperature range 1.3–300 K, which was extended down to 85 mK at the highest pressure. The magnitude of ρ at room temperature (RT) and ambient pressure was scaled to the value obtained in the previous work [6] because of the uncertainty in the estimation of the absolute value of ρ for the tiny samples ($\sim 0.8 \times 0.3 \times 0.2\ \mathrm{mm}^3$) used in the pressure cell. Hydrostatic pressure was applied by an indenter cell with Daphne oil 7474 as a pressure-transmitting medium [33,34]. The applied pressure value at low temperature was determined from the shift in the superconducting transition temperature of lead [35].

3. Results and discussions

Figs. 1(a) and (b) show the temperature dependence of the resistivity at various pressures ($P \le 4.47$ GPa) below 300 and 100 K, respectively. At approximately ambient pressure of 0.03 GPa, two kink anomalies can be seen at 16.2 K and 5.8 K, which correspond to T_Q and T_C, respectively. Here, T_Q and T_C were determined from a peak position of $-\mathrm{d}^2\rho/\mathrm{d}T^2$. Both the observed T_Q and T_C at this pressure are in good agreement with those given in the previous reports at ambient pressure [3,4]. At $P \sim 0.19$ GPa, the FQ transition is terminated suddenly by the structural phase transition from the cubic to tetragonal. The transition temperature T_{s1} of this first-order phase transition was determined from the midpoint of the hysteresis loop of $\rho(T)$ curves. T_{s1} starts at ~30 K ($P \sim 0.19$ GPa) and increases linearly with increasing pressure at a rate of $\mathrm{d}T_{s1}/\mathrm{d}P \sim 170$ K/GPa, which shows a good agreement with the values reported in the previous studies [5–8].

As pressure increases, T_{s1} is raised above RT, and another anomaly with a broader thermal hysteresis appears above ~2.3 GPa. This corresponds to the first-order phase transition at T_{s2}, which is believed to be another structural transition from the tetragonal to some other phase. T_{s2} was also defined as the midpoint of the hysteresis loop of $\rho(T)$. T_{s2} increases monotonously with increasing pressure, but it could not be determined above ~3.2 GPa because of disappearance of the $\rho(T)$ hysteresis.

It should also be noted that the absolute value of ρ increases with increasing pressure in the whole temperature range. Possible origin of this behavior would be a change in the band structure due to the structural change, an increase of scattering of the conduction electrons by domain formation due to the crystal distortion, and/or an enhancement of the Kondo effect by applying pressure. Interestingly, the $\rho(T)$ curve exhibits a shoulder at low temperatures below ~100 K in the second high-pressure phase above ~2.1 GPa, as can be seen in Fig. 1(b). This behavior is suggestive of development of a Kondo coherent state, whose characteristic temperature, named as T^*, was determined by the point of intersection for two linear extrapolations from the higher and lower temperatures in $\mathrm{d}\rho/\mathrm{d}T$, as represented in the inset of Fig. 1(b). Details of its pressure dependence will be discussed later.

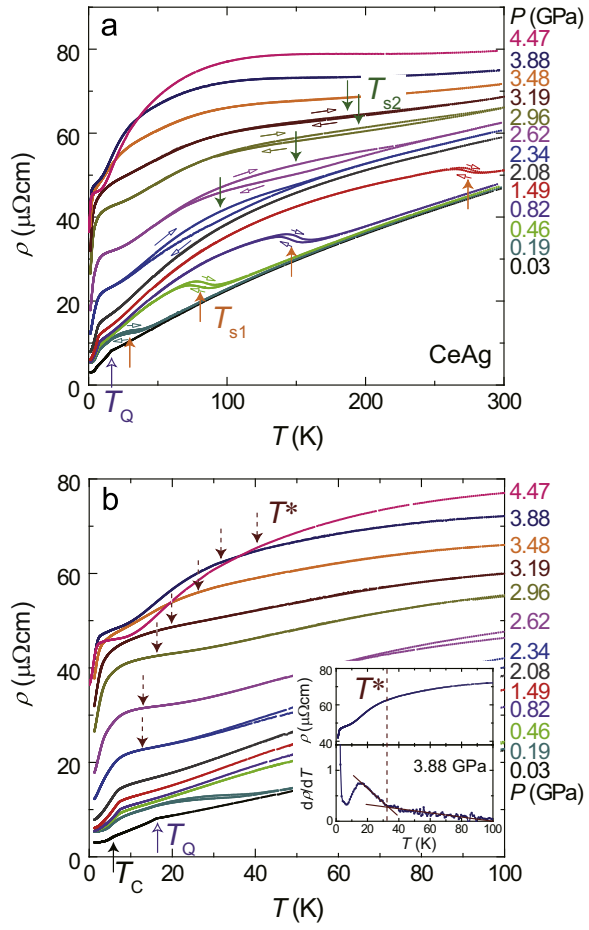

Fig. 1. (a) Temperature dependence of the electrical resistivity of CeAg at several pressures up to 4.47 GPa below 300 K. T_Q, T_{s1} and T_{s2} are represented by the open-upward, closed-upward and closed-downward arrows, respectively. The small open arrows indicate the cooling and heating processes at each pressure. (b) Enlarged view of $\rho(T)$ below 100 K. The closed-upward and dashed-downward arrows indicate T_C and T^*, respectively. The inset of Fig. 1(b) shows $\rho(T)$ and $\mathrm{d}\rho/\mathrm{d}T$ at 3.88 GPa. The lines are guides to the eye.

We converted $\rho(T)$ data measured at constant pressures to the pressure variations of the resistivity $\rho(P)$ at constant temperatures as shown in Fig. 2. The displayed data were shifted vertically for clarity. The data points for the cooling and heating processes are represented by closed and open symbols, respectively, though they show little difference. It can be seen that $\rho(P)$ exhibits a step-like increase in the low pressure region below 2 GPa. We define the 'transition pressure' P_{s1} as the midpoint of the step-like increase. On the other hand, above 2 GPa, we found another transition at P_{s2} appearing as a break in the $\rho(P)$ curves. Here, we determined P_{s2} by the point of intersection for the two linear extrapolations from the higher and lower pressure sides. P_{s1} and P_{s2} are both almost pressure-independent at low temperatures, while they start shifting to higher pressure side with increasing temperature above ~ 40 K. We could not determine P_{s2} in the $\rho(P)$ curves for temperatures higher than 200 K, where the break in $\rho(P)$ becomes quite obscure.

The results concerning the successive first-order phase transitions are summarized as a P–T phase diagram in Fig. 3(a). Closed and open symbols represent the data obtained from the temperature and pressure dependences of ρ, respectively. We also plotted the transition points obtained from our $\rho(T)$ measurements performed by using unannealed samples and Daphne oil 7373 as a pressure-transmitting medium. Hereafter we refer to the cubic, tetragonal, and unknown phases as Phases I, II, and III,